arXiv:hep-ph/9710420v1 21 Oct 1997

UL–NTZ 28/97

Helicity amplitudes for the small angle lepton pair production in e^+e^- or $\mu^+\mu^-$ collisions

E.A. Kuraev[1]*, A. Schiller[2]†, V.G. Serbo[3]‡and D.V. Serebryakova[4]
[1] Joint Institute of Nuclear Research, 141980, Dubna, Russia
[2] Institut für Theoretische Physik and Naturw.-Theoretisches Zentrum, Universität Leipzig, D-04109 Leipzig, Germany
[3] Novosibirsk State University, 630090, Novosibirsk, Russia
[4] Institute of Mathematics, 630090, Novosibirsk, Russia

October 21, 1997

Abstract

The lepton pair production $e^-e^+ \to e^-e^+l^-l^+$ or $\mu^-\mu^+ \to \mu^-\mu^+l^-l^+$ is studied in the dominant cross section region of scattering angles $m_j/E_j \lesssim \theta_j \ll 1$. An analytical expression is found for all 64 helicity amplitudes of these processes. The accuracy of the obtained formulae is given omitting only terms of the order of m_j^2/E_j^2, θ_j^2 and $\theta_j m_j/E_j$. The result has a compact form convenient both for analytical and numerical calculations of various cross sections in this dominating scattering regime.

1 Introduction

Colliders with electron and photon beams are now widely used or designed to study fundamental interactions. Among other QED reactions those inelastic processes are of special interest the cross section of which do not drop with increasing energies. To third and fourth orders in the electromagnetic coupling α these processes are shown in Figs. 1-8 (only block diagrams are presented). Figs. 1 and 2 describe the lepton pair production in γe and $\gamma\gamma$ collisions arising from $\gamma\gamma^*$ interactions. Figs. 3 and 4 correspond to single and double bremsstrahlung (with a single photon along its parent lepton), Fig. 5 and 6

*E-mail: kuraev@thsun1.jinr.dubna.su
†E-mail: schiller@tph204.physik.uni-leipzig.de
‡E-mail: serbo@math.nsc.ru

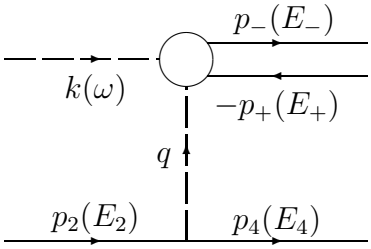

Figure 1: Reaction $\gamma e \to l^+ l^- e$

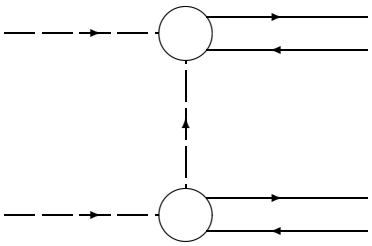

Figure 2: Reaction $\gamma\gamma \to e^+ e^- l^+ l^-$

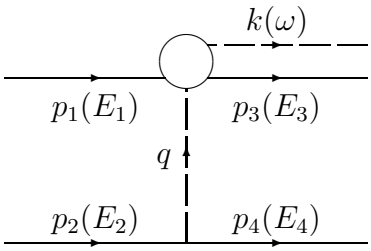

Figure 3: Single bremsstrahlung $ee \to ee\gamma$

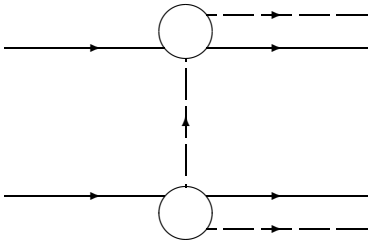

Figure 4: Double bremsstrahlung $ee \to ee\gamma\gamma$

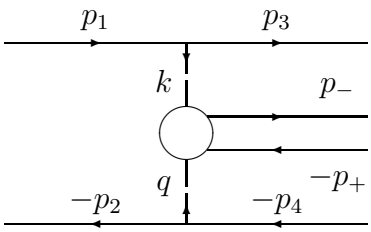

Figure 5: Two–photon pair production $e^- e^+ \to e^- e^+ l^- l^+$

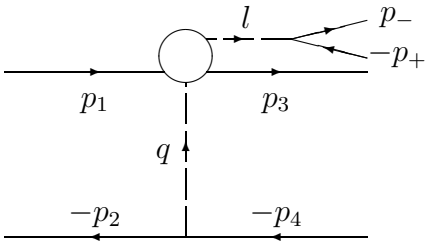

Figure 6: Bremsstrahlung pair production $e^- e^+ \to e^- e^+ l^- l^+$

to the lepton pair production by the two–photon and bremsstrahlung mechanisms, Fig. 7 gives the process $\gamma e \to l^+ l^- e\gamma$ and Fig. 8 the double bremsstrahlung along one direction.

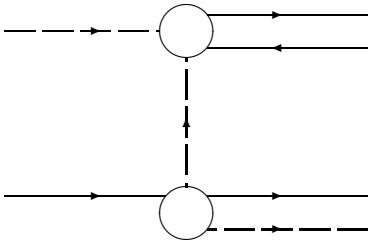

Figure 7: Reaction $\gamma e \to l^+ l^- e\gamma$

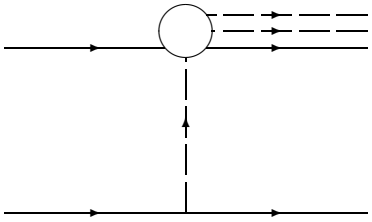

Figure 8: Double bremsstrahlung $ee \to ee\gamma\gamma$ in one direction

The described processes are important by the following reasons

(i) Some of these reactions are used (or are proposed to be used) as the monitoring processes to determine the collider luminosity and to measure the polarisation of the colliding particles. For example, the double bremsstrahlung Fig. 2 has been used as the

standard calibration process at several colliders in Novosibirsk, Frascati and Orsay [1]-[3]. In [4] it has been suggested to use the single bremsstrahlung Fig. 1 for measuring the luminosity and the polarisation of the initial $e^{\pm}$ at the LEP collider (see also the paper [5]). It has been demonstrated in an experiment [6] that this single bremsstrahlung process has a good chance to be used for luminosity purposes. Recently [7] the same process is proposed to measure the luminosity at the DAΦNE collider. The processes $\gamma\gamma \to \mu^+\mu^- e^+ e^-$ and $\gamma\gamma \to \mu^+\mu^-\mu^+\mu^-$ may be useful to monitor colliding $\gamma\gamma$ beams [8, 9, 10]. Finally, the possibility of designing $\mu^+\mu^-$ colliders is widely discussed [11] at present. Therefore, the processes $\mu^+\mu^- \to l^+l^-l^+l^-$ ($l = e, \mu$) may be useful for luminosity measurements at those colliders [12].

(ii) Due to their large cross sections those reactions contribute as a significant background to a number of experiments in the electroweak sector and to hadronic cross sections. For example, the background process $e^+e^- \to e^+e^-\mu^+\mu^-$ is of special importance for experiments studying the two–photon $\pi^+\pi^-$ production due to the known experimental difficulties in discriminating pions and muons.

(iii) The methods to calculate the helicity amplitudes of those processes and to obtain some distributions for them can be easily translated to several semihard QCD processes such as $\gamma\gamma \to q\overline{q}Q\overline{Q}$ [10] (q and Q are different quarks) and $\gamma\gamma \to MM'$, $\gamma\gamma \to Mq\overline{q}$ [13] (M, M' denote neutral mesons as ρ^0, ω, ϕ, Ψ, π^0, a_2...).

At high energies with the condition (m_j are the lepton masses)

$$s = 2p_1p_2 = 4E_1E_2 \gg m_j^2 \tag{1}$$

the dominant contribution to the cross sections of Figs. 1-8 are given by the region of scattering angles θ_j which are much smaller than unity though they may be of the order of the typical emission angles m_j/E_j or larger:

$$\frac{m_j}{E_j} \lesssim \theta_j \ll 1 \ . \tag{2}$$

In this region all processes have the form of two–jet processes with an exchange of a single virtual photon γ^* in the t–channel (see Fig. 9).

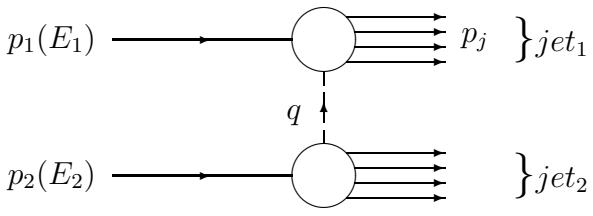

Figure 9: Generic block diagram $ee \to \mathrm{jet}_1\ \mathrm{jet}_2$

The considered QED processes are widely discussed in the literature. Taking into account unpolarised leptons and photons only, various differential cross sections are summarised in reviews [14] and [15]. Recently the considered reactions have been taken into account as radiative corrections to the unpolarised Bhabha scattering used as calibration process at LEP [16].

In the nearest future beams with polarised leptons and photons will be available which demands to calculate cross sections with polarised particles. In this connection we would like to note that in the kinematic region (1-2) the discussed QED processes can be found in a "final form" including the polarisations of all particles. By this we mean that it is possible to obtain compact and simple analytical expressions for all helicity amplitudes with high accuracy. Omitting terms of the order of

$$\frac{m_j^2}{E_j^2}\ ,\quad \theta_j^2\ ,\quad \frac{m_j}{E_j}\theta_j \tag{3}$$

only, the amplitude M_{fi} of any process given in Figs. 1-8 can be represented in a simple factorised form

$$M_{fi} = \frac{s}{q^2} J_1 J_2\ . \tag{4}$$

The vertex factor J_1 (J_2) corresponds to the first jet or upper block (second jet or lower block) of Fig. 9. The factor $J_{1(2)}$ depends on the energy fraction $x_j = E_j/E_{1(2)}$, the transverse momenta $\mathbf{p}_{j\perp}$, the helicities λ_i of the particles in the first (second) jet and the helicity $\lambda_{1(2)}$ of the initial particle with 4–momentum $p_{1(2)}$. The function $J_{1(2)}$ is independent on the cms energy squared s.

This approximation differs considerably from the known results of the CALCUL group and others [17, 18] where such processes are calculated for not too small scattering angles of the final particles. This allows to neglect completely lepton masses, i.e. neglecting the terms of the order of $m_j/|\mathbf{p}_{j\perp}|$, which, however, give the dominant contribution to the total cross section at small angles.

For the reactions of Figs. 1-4,7 the corresponding vertex factors and some differential cross sections have been found in [9, 10, 19]. These vertex factors are presented in Sec. 2 and partly used below, too.

In the present paper we give a complete set of helicity amplitudes for the lepton pair production at $e^{\pm}e^-$ and $\mu^{\pm}\mu^-$ colliders (see Figs. 5 and 6) in the region (1-2). For definiteness, we consider the process

$$e^-e^+ \to e^-e^+\mu^-\mu^+\ . \tag{5}$$

In Sec. 3 we derive the vertex factors necessary to calculate the transition amplitude of the two–photon lepton pair production of Fig. 5. The following Section is devoted to the pair production via bremsstrahlung. In Sec. 5 our results are briefly summarised and qualitative features of cross sections are discussed.

To complete the jet–like QED tree processes to fourth order, the double bremsstrahlung along one jet direction has to be calculated for the kinematic region under discussion. This work is now in progress.

Let us introduce some notations using the block diagram of Fig. 9 as an example. We use a reference frame in which the initial particles with 4–momenta p_1 and p_2 perform a head–on collision with energies E_1 and E_2 of the same order (e.g. at the B–factory). The z–axis is chosen along the momentum $\mathbf{p}_1$, the azimuthal angles are denoted by φ_i (they

are referred to one fixed x-axis). It is convenient to introduce "the almost light–like" 4–vectors p and p'

$$p = p_1 - \frac{m^2}{s}\, p_2,\ p' = p_2 - \frac{m^2}{s}\, p_1,\ p^2 = {p'}^2 = \frac{m^6}{s^2},$$

$$s = 2p_1p_2 = 2pp' + \frac{3m^4}{s}\,. \tag{6}$$

Throughout the paper we use the notation $\mathbf{Q}$ and R which enter in the definition of the vertex factors

$$\mathbf{Q} = \frac{\mathbf{u}}{a} + \frac{\mathbf{v}}{b},\quad R = \frac{1}{a} - \frac{1}{b}\,,\quad \mathbf{u} + \mathbf{v} = \mathbf{q}_\perp\,,\quad b - a = \mathbf{v}^2 - \mathbf{u}^2\,. \tag{7}$$

$\mathbf{q}_\perp$ denotes the transverse momentum of the t–channel virtual photon. The quantities $\mathbf{u}$, $\mathbf{v}$, a and b are process dependent. Note the following useful relation between $\mathbf{Q}^2$ and R^2

$$\mathbf{Q}^2 + (a - \mathbf{u}^2)R^2 = \frac{\mathbf{q}_\perp^2}{ab}\,. \tag{8}$$

Additionally, the helicity vectors

$$\mathbf{e}_\lambda = -\frac{\lambda}{\sqrt{2}}(1, i\lambda, 0) = -\mathbf{e}^*_{-\lambda},\quad \lambda = \pm 1 \tag{9}$$

are used to describe the photon polarisation.

2 A short description of our previous results

The amplitude M_{fi} corresponding to the diagram of Fig. 9 can be presented in the form

$$M_{fi} = M_1^\mu\, \frac{g_{\mu\nu}}{q^2}\, M_2^\nu, \tag{10}$$

where M_1^μ and M_2^ν are the amplitudes of the upper and lower block of Fig. 9, respectively, $(-g_{\mu\nu}/2)$ denotes the density matrix of the virtual photon. The transition amplitude M_1 describes the scattering of an incoming lepton or photon with a virtual photon of "mass" squared q^2 and polarisation vector $\mathbf{e} = \mathbf{q}_\perp/|\mathbf{q}_\perp|$ to some QED final state in the jet kinematics (1-2) (similar for M_2).

With accuracy (3) the $g_{\mu\nu}$ matrix can be transformed to the form

$$g_{\mu\nu}\ \to \frac{2}{s}\, p'_\mu\, p_\nu \tag{11}$$

(for detail see [20], §4.8.4) which results in Eq. (4). The vertex factors $J_{1,2}$ are given by the block amplitudes $M^\mu_{1,2}$

$$M_{fi} = \frac{s}{q^2}\, J_1\, J_2,\quad J_1 = \frac{\sqrt{2}}{s}\, M_1^\mu\, p'_\mu,\quad J_2 = \frac{\sqrt{2}}{s}\, M_2^\mu\, p_\mu\,. \tag{12}$$

The quantities J_1 and J_2 can be calculated in the limit $s \to \infty$ assuming that the energy fractions and transverse momenta of the final particles $\mathbf{p}_{i\perp}$ are finite in this limit. For the convenience of the reader we present in the following the vertex factors corresponding to processes of Figs. 1-4 taken from Refs. [10, 19].

The vertex factor $J_1(e^{\pm}_{\lambda_1} \to e^{\pm}_{\lambda_3})$ describing the transition of a $e^{\pm}$ with momentum p_1 and helicity λ_1 to a $e^{\pm}$ with momentum p_3 and helicity λ_3 (Fig. 10) is equal to

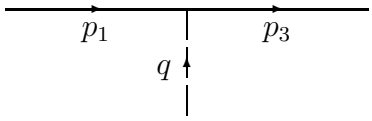

Figure 10: Amplitude $e^-\gamma^* \to e^-$ for $J_1(e^-_{\lambda_1} \to e^-_{\lambda_3})$

$$J_1(e^{\pm}_{\lambda_1} \to e^{\pm}_{\lambda_3}) = \sqrt{8\pi\alpha}\,\delta_{\lambda_1\lambda_3}\,\mathrm{e}^{i(\lambda_3\varphi_3-\lambda_1\varphi_1)}\,. \tag{13}$$

This vertex contributes to the transition amplitudes of Figs. 1, 3, 5, 6 and 8. Its derivation is presented in detail in Sec. 3.2. The azimuthal angle of the initial state lepton φ_1 can be chosen equal to zero.

The vertex factor for the transition of a real photon with energy ω and helicity λ into a lepton pair (Fig. 11, which corresponds to the upper block of Figs. 1, 2, 7 and lower

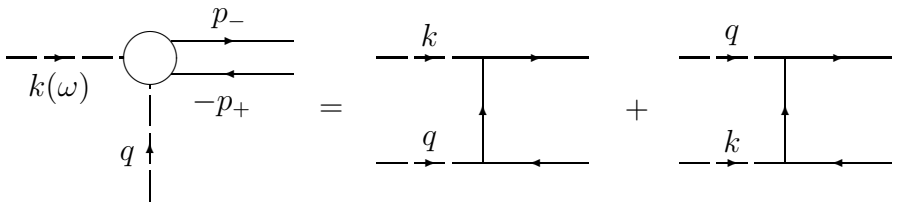

Figure 11: Amplitude $\gamma\gamma^* \to l^+l^-$ for $J_1(\gamma_\lambda \to e^+_{\lambda_+}e^-_{\lambda_-})$

block of Fig. 2) is equal to

$$\begin{aligned} J_1(\gamma_\lambda \to e^+_{\lambda_+}e^-_{\lambda_-}) \;&=\; i4\pi\alpha\,\sqrt{x_+x_-}\,\Big[(x_+-x_-+2\lambda_+\lambda)\sqrt{2}\mathbf{Q}\mathbf{e}_\lambda\,\delta_{\lambda_+,-\lambda_-} - \\ &\quad -2mR\delta_{\lambda_+,\lambda_-}\,\delta_{\lambda,2\lambda_+}\Big]\,\mathrm{e}^{i(\lambda_+\varphi_+ +\lambda_-\varphi_-)}\,, \end{aligned} \tag{14}$$

where $x_\pm = E_\pm/\omega$ are the lepton energy fractions. The quantities $\mathbf{Q}$ and R are defined in (7) with

$$\mathbf{u} = \mathbf{p}_{+\perp}\,,\quad \mathbf{v} = \mathbf{p}_{-\perp}\,,\quad a = m^2+\mathbf{u}^2,\quad b = m^2+\mathbf{v}^2. \tag{15}$$

The vertex factor for the transition of an electron or positron $e^{\pm}$ to $e^{\pm}$ and a photon with momentum (energy) $k(\omega)$ and helicity λ (Fig. 12, appearing in the upper block of

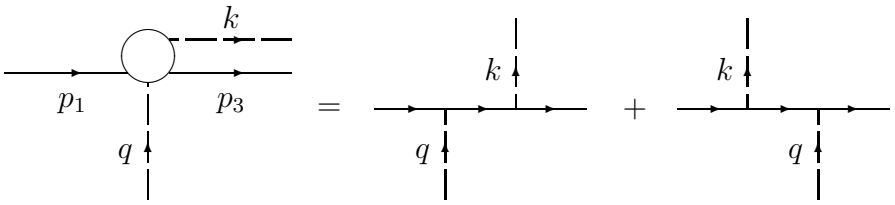

Figure 12: Amplitude $e^-\gamma^* \to e^-\gamma$ for $J_1(e^-_{\lambda_1} \to e^-_{\lambda_3}\,\gamma_\lambda)$

Figs. 3, 4 and lower block of Fig. 7) is given by

$$J_1(e^\pm_{\lambda_1} \to e^\pm_{\lambda_3}\,\gamma_\lambda) \;=\; \pm 4\pi\alpha\,\sqrt{1-x}\left[\left(\frac{2-x}{x}+2\lambda_1\lambda\right)\sqrt{2}\mathbf{Q}\mathbf{e}_{-\lambda}\delta_{\lambda_1\lambda_3} - \right.$$
$$\left. - \,2mR\delta_{\lambda_1,-\lambda_3}\,\delta_{\lambda,2\lambda_1}\right]\,\mathrm{e}^{i(\lambda_3\varphi_3-\lambda_1\varphi_1)}\,, \qquad (16)$$

where $x = \omega/E_1$. The quantities $\mathbf{Q}$ and R are of form (7), however

$$\mathbf{u} = \frac{\mathbf{k}_\perp}{x}\,,\;\; \mathbf{v} = \mathbf{q}_\perp - \frac{\mathbf{k}_\perp}{x},\;\; a = m^2 + \mathbf{u}^2,\;\; b = m^2 + \mathbf{v}^2. \qquad (17)$$

Again the azimuthal angle φ_1 can be set equal to zero. Note the useful relation for quantities $\mathbf{Q}$ and R valid for relations (15) and (17)

$$\mathbf{Q}^2 + m^2R^2 = \frac{\mathbf{q}^2_\perp}{ab}\,. \qquad (18)$$

The amplitude of Fig. 12 is the cross amplitude to that of Fig. 11. Therefore, the corresponding vertex factors are connected by the relation

$$J_1(\gamma \to e^+e^-) \to -\frac{J_1(e \to e\gamma)}{x} \qquad (19)$$

using the substitution rules

$$\mathbf{p}_{+\perp} \to \frac{\mathbf{k}_\perp}{x}\;,\;\; \mathbf{p}_{-\perp} \to \mathbf{q}_\perp - \frac{\mathbf{k}_\perp}{x}\;,\;\; x_+ \to \frac{1}{x}\;,\;\; x_- \to -\frac{1-x}{x}\,, \qquad (20)$$

$$\lambda \to -\lambda\;,\;\; \lambda_+ \to -\lambda_1\;,\;\; \lambda_- \to \lambda_3\;,\;\; \varphi_{+,-} \to \varphi_{1,3}\;. \qquad (21)$$

Here relations (20) are known substitution rules for the unpolarised cross sections [21]. Taking into account the polarisation of the particles, relations (21) describe additional substitution rules to be added to (20).

Both vertex factors have a symmetry related to the obvious symmetry of Fig. 11 under lepton exchange $l^+ \leftrightarrow l^-$. The vertex factor $J_1(\gamma \to e^+e^-)$ (14) changes its sign under the replacements $+ \leftrightarrow -$. Analogously, the vertex factor $J_1(e \to e\gamma)/\sqrt{1-x}$ (16) changes its sign under

$$\mathbf{u} \leftrightarrow \mathbf{v},\;\; x \leftrightarrow -\frac{x}{1-x}\,,\;\; \lambda_1 \leftrightarrow -\lambda_3\,,\;\; \varphi_1 \leftrightarrow \varphi_3\,. \qquad (22)$$

Eqs. (12)-(17) completely describe all helicity amplitudes of Figs. 1-4 and 7. They are not only very compact expressions but they are also convenient for numerical calculations.

The reason is that in their form large compensating terms are already cancelled. Indeed, looking for the behaviour of $\mathbf{Q}$ and R in the limit of vanishing $\mathbf{q}_\perp$ one immediately finds that (compare with Eq. (18))

$$|\mathbf{Q}|,\ R \propto |\mathbf{q}_\perp| \ \text{ at } \ |\mathbf{q}_\perp| \to 0\ . \tag{23}$$

This completes the summary of previous results.

3 Two photon mechanism for the lepton pair production

3.1 Sudakov variables

Let us consider the block diagram of Fig. 5. The 4–momenta (energies) of the final electron and positron are denoted by $p_3(E_3)$ and $p_4(E_4)$, respectively, those of the produced muons $\mu^\mp$ by $p_\mp(E_\mp)$. The azimuthal angles of the final particles are $\varphi_{3,4,\pm}$, the polar angles of the final electron and muons with respect to the z-axis are $\theta_{3,\pm}$, the polar angles of the final positron with respect to the $(-z)$-axis is θ_4. The electron and the muon mass are denoted by m and M, respectively.

There are three different kinematic regions to be distinguished:

1. Electron fragmentation region
   The particles in the produced pair move along the initial electron direction (inside the first jet) with energy $\sim E_1$, and the scattered positron loses a small fraction of its energy. If we introduce the energy fractions of the final particles as

   $$x_{3,\pm} = \frac{E_{3,\pm}}{E_1}\ , \quad x = x_+ + x_-\ , \tag{24}$$

   these quantities are of the order of 1.

2. Positron fragmentation region
   It is obtained from the electron fragmentation region by substituting $e^- \leftrightarrow e^+$.

3. Region of soft particle production
   In that region $x_\pm \ll 1$, this case will be discussed in Sec. 5.

Throughout the paper we treat the electron fragmentation region in detail.

Let us introduce the 4-momenta $k = p_1 - p_3$ of the virtual photon γ_k^* inside block J_1 and $q = p_2 - p_4$ of the virtual photon γ^* connecting the blocks J_1 and J_2. We decompose the 4–vectors p_i $(i = 1 - 4, \pm)$, k and q into components in the plane of the 4–vectors p and p' (see (6)) and in the plane orthogonal to them

$$\begin{aligned} p_i &= \alpha_i p' + \beta_i p + p_{i\perp}\ , \\ k = p_1 - p_3 &= \alpha_k p' + \beta_k p + k_\perp\ , \\ q = p_2 - p_4 &= \alpha_q p' + \beta_q p + q_\perp\ . \end{aligned} \tag{25}$$

The parameters α and β are the so called Sudakov parameters. In the used reference frame the 4–vectors $p_{i\perp}$, $k_\perp$ and $q_\perp$ have x and y components only, e.g.

$$q_\perp = (0,\, q_x,\, q_y,\, 0) = (0,\, \mathbf{q}_\perp,\, 0)\,, \quad q_\perp^2 = -\mathbf{q}_\perp^2\,. \tag{26}$$

In this jet–like kinematics we note the useful relation

$$p_j^2 = m_j^2 = s\alpha_j\beta_j - \mathbf{p}_{j\perp}^2\,. \tag{27}$$

for the final state particles (in our case $j = 3, 4, \pm$) which is valid in general. The 4–vectors p_l of particles from the first jet (here $l = 3, \pm$) obtain large components along p_1 and small ones along p_2. Therefore, in the limit $s \to \infty$ (with accuracy (3)) the quantities $\beta_l = 2p_lp'/s = E_l/E_1$ are finite whereas $\alpha_l = 2p_lp/s = (m_l^2 + \mathbf{p}_{l\perp}^2)/(s\beta_l)$ are small[1].

In particular, for our case of the electron fragmentation region (block diagram of Fig. 5, $l = 3, \pm$) the Sudakov parameters

$$\beta_1 = 1,\ \beta_l = x_l,\ \alpha_2 = 1,\ \alpha_4 = \alpha_2 - \alpha_q \approx 1,\ \beta_k = \beta_1 - \beta_3 = 1 - x_3 \approx x \tag{28}$$

are finite at $s \to \infty$, whereas the parameters

$$\alpha_1 = \frac{m^2}{s},\ \alpha_l = \frac{m_l^2 + \mathbf{p}_{l\perp}^2}{sx_l},\ \beta_2 = \frac{m^2}{s},\ \beta_4 = \frac{m^2 + \mathbf{p}_{4\perp}^2}{s},$$

$$\alpha_k = \alpha_1 - \alpha_3,\ \alpha_q = \alpha_+ + \alpha_- + \alpha_3 - \alpha_1,\ \beta_q = \beta_2 - \beta_4 \tag{29}$$

are small. Therefore, the energy of the final and initial positrons are approximately equal $E_4 \approx E_2$. The energy fractions x and x_l are defined in Eq. (24).

Next, we derive a useful expression for the virtualities k^2 and q^2. From the obvious relations $(p_1 - k)^2 = p_3^2$ and $(p_2 - q)^2 = p_4^2$ or $2p_1k = s\alpha_k + m^2\beta_k = k^2 = s\alpha_k\beta_k - \mathbf{k}_\perp^2$ and $2p_2q = s\beta_q + m^2\alpha_q = q^2 = s\alpha_q\beta_q - \mathbf{q}_\perp^2$ we obtain

$$k^2 = -\frac{\mathbf{k}_\perp^2 + m^2\beta_k^2}{1 - \beta_k}\,,\ \ q^2 = -\frac{\mathbf{q}_\perp^2 + m^2\alpha_q^2}{1 - \alpha_q}\,. \tag{30}$$

According to Eqs. (12) the amplitude $e^-e^+ \to e^-e^+\mu^-\mu^+$ for this kinematics has the form (4) where the vertex factors J_1 and J_2 have to be determined.

3.2 Calculation of J_2

To clarify some points in the further calculations we start with a detailed derivation of the vertex factor J_2 (Fig. 13) which is equal to

$$J_2(e^+_{\lambda_2} \to e^+_{\lambda_4}) = \frac{\sqrt{8\pi\alpha}}{s}\bar v_2\,\hat p\,v_4\,. \tag{31}$$

[1] Analogously, for a 4–vector p_l (here $l = 4$) of a particle from the second jet the quantity $\alpha_l = E_l/E_2$ is finite, $\beta_l = (m_l^2 + \mathbf{p}_{l\perp}^2)/(s\alpha_l)$ is small.

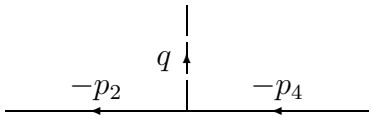

Figure 13: Amplitude $e^+\gamma^* \to e^+$ for $J_2(e^+_{\lambda_2} \to e^+_{\lambda_4})$

The spinor v_j $(j = 2, 4)$ corresponds to a positron with 4-momentum p_j and helicity λ_j. Using the explicit formulae for spinors (see Appendix A) we have

$$J_2 = \frac{\sqrt{8\pi\alpha}}{s}\, E_1 \left(\sqrt{E_2+m}+\sqrt{E_2-m}\right)\left[\left(\sqrt{E_4+m}+\sqrt{E_4-m}\right)\cos\frac{\theta_4}{2}\,\mathrm{e}^{-i\lambda_4\varphi_4}\,\delta_{\lambda_2\lambda_4}+\right.$$
$$\left.+2\lambda_2\left(\sqrt{E_4+m}-\sqrt{E_4-m}\right)\sin\frac{\theta_4}{2}\,\mathrm{e}^{i\lambda_4\varphi_4}\,\delta_{\lambda_2,-\lambda_4}\right]. \qquad (32)$$

This expression is simplified by omitting terms of the order $O(m^2/E_j^2)$ while keeping terms of the order $O(m/E_j)$

$$J_2 = \sqrt{8\pi\alpha}\left[\cos\frac{\theta_4}{2}\mathrm{e}^{-i\lambda_4\varphi_4}\,\delta_{\lambda_2\lambda_4}+\lambda_2\frac{m}{E_4}\,\sin\frac{\theta_4}{2}\,\mathrm{e}^{i\lambda_4\varphi_4}\,\delta_{\lambda_2,-\lambda_4}\right]. \qquad (33)$$

Note that in the considered region of small angles (2), the term $\sim m/E_4$ has an additional smallness $\sim \theta_4$. Therefore, omitting terms of the order $O(m\theta_4/E_4, \theta_4^2/E_4^2)$ (Eq. (3)) we finally obtain for the vertex factor of the lower block

$$J_2 = \sqrt{8\pi\alpha}\,\mathrm{e}^{-i\lambda_4\varphi_4}\,\delta_{\lambda_2\lambda_4} \qquad (34)$$

from which it follows that the positron conserves its helicity. The origin of the different sign in the exponent compared to Eq. (13) is the positron moving opposite to the direction of the z-axis.

3.3 Calculation of J_1

We present the vertex factor J_1 (Fig. 14) of the two–photon lepton pair production from

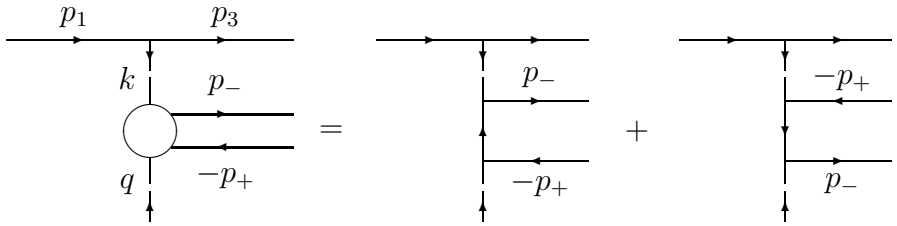

Figure 14: Two–photon pair production amplitude $e^-\gamma^* \to e^-\mu^+\mu^-$ for $J_1(e^-_{\lambda_1} \to e^-_{\lambda_3}\mu^+_{\lambda_+}\mu^-_{\lambda_-})$

Eq. (12) in the form

$$J_1(e^-_{\lambda_1} \to e^-_{\lambda_3}\mu^+_{\lambda_+}\mu^-_{\lambda_-}) = \frac{\sqrt{2}}{s}\,\frac{(4\pi\alpha)^{3/2}}{k^2}\,\bar{u}_-\left[\frac{\hat{p}'(\hat{k}-\hat{p}_+ + M)\hat{I}}{2kp_+ - k^2}+\frac{\hat{I}(\hat{p}_- - \hat{k}+M)\hat{p}'}{2kp_- - k^2}\right]v_+\,, \qquad (35)$$

where the expression in square brackets corresponds to the amplitude of the $\gamma_k^*\gamma^* \to \mu^+\mu^-$ process of Fig. 11 with two virtual photons. The 4–vector

$$I_\mu = \bar{u}_3 \gamma_\mu u_1 \tag{36}$$

is the current of the $e^- \to e^-\gamma_k^*$ transition. Comparing J_1 (Eq. (35)) with the corresponding expression needed in the usual photoproduction $\gamma e \to \mu^+\mu^- e$ of Fig. 1

$$J_1(\gamma_\lambda \to \mu^+_{\lambda_+}\mu^-_{\lambda_-}) = \frac{\sqrt{2}}{s} 4\pi\alpha \; \bar{u}_- \left[\frac{\hat{p}'(\hat{k} - \hat{p}_+ + M)\hat{e}}{2kp_+} + \frac{\hat{e}(\hat{p}_- - \hat{k} + M)\hat{p}'}{2kp_-} \right] v_+ \tag{37}$$

we note two significant differences:
(i) In the process of Fig. 5 the photon γ_k^* with 4–momentum k is virtual, $k^2 \neq 0$, while in the usual photoproduction this photon is real, $k^2 = 0$;
(ii) In the photoproduction J_1 includes the photon polarisation vector e_μ while in the process of Fig. 5 the vertex factor J_1 includes the quantity $\sqrt{4\pi\alpha} I_\mu / k^2$.
In the further calculation we follow the scheme developed in Refs. [10], [19] taking into account the noticed differences.

In order to calculate the vertex J_1 it is convenient (using gauge invariance) to replace the current I_μ by the 4–vector V_μ which has no component along p (just as in photoproduction where we can choose e_μ in the form $e_\mu = e_{\mu\perp}$)

$$I_\mu \to V_\mu = I_\mu - \frac{\beta_I}{\beta_k} k_\mu = \alpha_V \, p'_\mu + V_{\perp\mu} \, . \tag{38}$$

since $\beta_V = 2Vp'/s = 0$. Consequently, in the final expression only $V_\perp$ enters.

Using the Sudakov decomposition of Sec. 3.1 the denominators in Eq. (35) can be transformed to

$$2kp_\pm - k^2 = \frac{x}{x_\pm} \left(M^2 + \mathbf{r}_\pm^2 - \frac{x_+ x_-}{x^2} \, k^2 \right) \tag{39}$$

with

$$r^\mu_\pm = p^\mu_{\pm\perp} - \frac{x_\pm}{x} \, k^\mu_\perp \, , \quad \mathbf{r}_+ + \mathbf{r}_- = \mathbf{q}_\perp \, . \tag{40}$$

It is useful to note that the vectors $\mathbf{r}_+$ and $\mathbf{r}_-$ (corresponding to the vectors $\mathbf{u}$ and $\mathbf{v}$ in Eq. (44) below) are the components of the vectors $\mathbf{p}_+$ and $\mathbf{p}_-$ transverse to the vector $\mathbf{k}$ in full analogy with the corresponding Eq. (15) for the photoproduction of Fig. 1.

In the numerator of the first term $N = \bar{u}_- \hat{p}'(\hat{k} - \hat{p}_+ + M)\hat{V} v_+$ the matrix $\hat{V}$ is transposed to the left, and using the Dirac equation $(\hat{p}_+ + M) \, v_+ = 0$ we obtain

$$N = \bar{u}_- \hat{p}' \, [2V(k - p_+) - \hat{V} \, \hat{k}] \, v_+ \, . \tag{41}$$

Taking into account

$$2V(k - p_+) = -2V_\perp r_+ - 2\frac{x_-}{x^2} \, \beta_I \, k^2$$

and

$$\hat{p}' \, \hat{V} \, \hat{k} \, v_+ = -\frac{x}{x_+} \hat{p}' \, \hat{V}_\perp (\hat{r}_+ + M) \, v_+$$

we transform N to

$$N = \frac{x}{x_+}\bar{u}_-\,\hat{p}'\left[-\frac{2x_+}{x}V_\perp r_+ + \hat{V}_\perp(\hat{r}_+ + M) - 2\frac{x_+x_-}{x^3}\,\beta_I\,k^2\right]v_+\,. \tag{42}$$

With similar transformations for the second term we find the vertex factor J_1 in the compact form

$$J_1 = \sqrt{2}\,\frac{(4\pi\alpha)^{3/2}}{s\,k^2}\,\bar{u}_-\hat{p}'\Lambda v_+\,,$$

$$\Lambda = 2\,\frac{x_+}{x}\,\mathbf{V}_\perp\mathbf{Q} + \hat{V}_\perp(\hat{Q} + MR) - 2\frac{x_+x_-}{x^3}\,\beta_I\,R\,k^2 \tag{43}$$

with

$$\mathbf{u} = \mathbf{r}_+\,,\ \mathbf{v} = \mathbf{r}_-\,,\ a = M^2 + \mathbf{u}^2 - \frac{x_+x_-}{x^2}\,k^2\,,\ b = M^2 + \mathbf{v}^2 - \frac{x_+x_-}{x^2}\,k^2\,. \tag{44}$$

The 4–vector Q in the considered reference frame has transverse components only $Q = (0, \mathbf{Q}, 0)$ and the quantities $\mathbf{Q}$ and R are defined in Eq. (7). Note the relation (see Eq. (8) and compare with Eq. (18))

$$\mathbf{Q}^2 + \left(M^2 - \frac{x_+x_-}{x^2}\,k^2\right)\,R^2 = \frac{\mathbf{q}_\perp^2}{ab}\,. \tag{45}$$

To prove the independence of J_1 on s, we use the explicit formulae for the spinors u_- and v_+ and omit terms of the order of (3) (just as it was done in Eqs. (33)-(36)). Moreover, to get a simple final expression for the helicity amplitudes, it is useful to introduce the helicity eigenvectors $\mathbf{e}_\lambda$ (9) and to decompose the vector $\mathbf{V}_\perp$ in the helicity basis $\mathbf{e}_\lambda$

$$\mathbf{V}_\perp = \sum_{\lambda=\pm1}(\mathbf{V}_\perp\mathbf{e}_\lambda^*)\,\mathbf{e}_\lambda = -\sum_{\lambda=\pm1}(\mathbf{V}_\perp\mathbf{e}_{-\lambda})\,\mathbf{e}_\lambda\ . \tag{46}$$

As a result, we obtain with accuracy (3)

$$J_1 = i\,(4\pi\alpha)^{3/2}\frac{\sqrt{x_+x_-}}{k^2}\,\mathrm{e}^{i(\lambda_+\varphi_+ + \lambda_-\varphi_-)}\times$$

$$\times\left\{\sum_\lambda(\mathbf{V}_\perp\mathbf{e}_\lambda^*)\left[\left(\frac{x_+ - x_-}{x} + 2\lambda_+\lambda\right)\sqrt{2}\mathbf{Q}\mathbf{e}_\lambda\delta_{\lambda_+,-\lambda_-} - 2MR\delta_{\lambda_+\lambda_-}\delta_{\lambda,2\lambda_+}\right] - \right.$$

$$\left. -2\sqrt{2}\,\frac{x_+x_-}{x^3}\,\beta_I\,R\,k^2\delta_{\lambda_+,-\lambda_-}\right\}\,. \tag{47}$$

For vanishing virtuality ($k^2 \to 0$) the expression in the square brackets of this equation coincides with the corresponding expression in Eq. (14) by identifying $x = 1$.

The result (47) can be presented with the same accuracy in another form using the two-component spinors w_{λ_j} in which we have to put the polar scattering angles of muons equal to zero ($\theta_\pm = 0$)

$$J_1 = i\sqrt{2}(4\pi\alpha)^{3/2}\frac{\sqrt{x_+x_-}}{k^2}\times$$

$$\times\,w_{\lambda_-}^+\left\{\frac{x_+ - x_-}{x}\mathbf{Q}\mathbf{V}_\perp + i\boldsymbol{\sigma}[\mathbf{Q} + MR\,\mathbf{n}_1, \mathbf{V}_\perp] - 2\,\frac{x_+x_-}{x^3}\,\beta_I\,R\,k^2\right\}w_{-\lambda_+} \tag{48}$$

with the Pauli matrices $\boldsymbol{\sigma}$ and the unit vector

$$\mathbf{n}_1 = \frac{\mathbf{p}_1}{|\mathbf{p}_1|}\,. \tag{49}$$

The only quantities which remain to be calculated are β_I and $\mathbf{V}_\perp \mathbf{e}^*_\lambda$. Setting the azimuthal angle of the incoming electron equal to zero ($\varphi_1 = 0$) we find

$$\beta_I = \frac{2}{s}\, p'_\mu I^\mu = \frac{2}{s}\bar{u}_3 \hat{p}' u_1 = 2\sqrt{1-x}\ \mathrm{e}^{i\lambda_3\varphi_3}\ \delta_{\lambda_1\lambda_3}\,, \tag{50}$$

and

$$\mathbf{V}_\perp \mathbf{e}^*_\lambda = -\lambda\sqrt{2E_1E_3}\,\mathrm{e}^{i\lambda_3\varphi_3}\times$$
$$\times\left[\left(\frac{1-x}{x}+\delta_{\lambda,2\lambda_1}\right)\theta_3\mathrm{e}^{-i\lambda\varphi_3}\,\delta_{\lambda_1\lambda_3}+\lambda\left(\frac{m}{E_3}-\frac{m}{E_1}\right)\delta_{\lambda,2\lambda_1}\ \delta_{\lambda_1,-\lambda_3}\right]. \tag{51}$$

The corresponding expressions suitable for crossing can be obtained by holding the energy fraction $x_1(=1)$, the polar $\theta_1(=0)$ and azimuthal $\varphi_1(=0)$ angles of the incoming electron as free parameters. In that case one obtains ($x_3 = 1-x$)

$$\beta_I = 2\sqrt{x_1x_3}\ \mathrm{e}^{i(\lambda_3\varphi_3-\lambda_1\varphi_1)}\ \delta_{\lambda_1\lambda_3}\,, \tag{52}$$

$$\mathbf{V}_\perp \mathbf{e}^*_\lambda = -\mathbf{V}_\perp \mathbf{e}_{-\lambda} = -\lambda\sqrt{2E_1E_3}\,\mathrm{e}^{i(\lambda_3\varphi_3-\lambda_1\varphi_1)}\times$$
$$\times\left\{\left[\left(\frac{x_1}{x}+\delta_{\lambda,-2\lambda_1}\right)\theta_1\,\mathrm{e}^{-i\lambda\varphi_1}+\left(\frac{x_3}{x}+\delta_{\lambda,2\lambda_1}\right)\theta_3\,\mathrm{e}^{-i\lambda\varphi_3}\right]\delta_{\lambda_1\lambda_3}-\right. \tag{53}$$
$$\left.-\lambda\left(\frac{m}{E_3}-\frac{m}{E_1}\right)\delta_{\lambda,2\lambda_1}\ \delta_{\lambda_1,-\lambda_3}\right\}.$$

The newly calculated vertex factor J_1 has again a symmetry related to the obvious symmetry of Fig. 14 under lepton exchange $\mu^+ \leftrightarrow \mu^-$. It changes its sign when replacing indices $+ \leftrightarrow -$.

4 Bremsstrahlung mechanism for the lepton pair production

Let us consider the block diagram of Fig. 6. The corresponding amplitude has the form (12) where the vertex factor J_2 is the same as in Eq. (34). The vertex factor J_1 (Fig. 15) we present in the form

$$J_1(e^-_{\lambda_1}\to e^-_{\lambda_3}\mu^+_{\lambda_+}\mu^-_{\lambda_-}) = \frac{\sqrt{2}}{s}\,\frac{(4\pi\alpha)^{3/2}}{l^2}\,\bar{u}_3\left[\frac{\hat{p}'(-\hat{l}+\hat{p}_1+m)\hat{I}}{2lp_1-l^2}+\frac{\hat{I}(\hat{p}_3+\hat{l}+m)\hat{p}'}{-2lp_3-l^2}\right]u_1 \tag{54}$$

where the expression in square brackets corresponds to the amplitude of the Compton scattering of the type of Fig. 12 with the virtual initial photon q and the virtual final photon

$$l = p_+ + p_- = \alpha_l p' + \beta_l p + l_\perp\,.$$

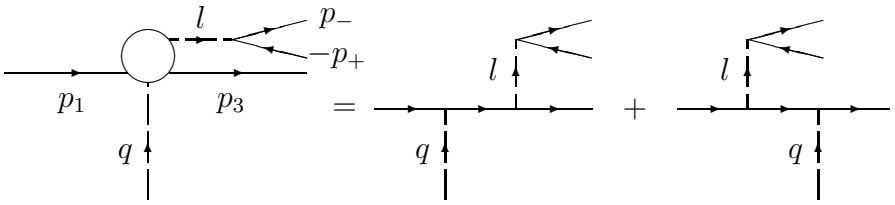

Figure 15: Bremsstrahlung pair production amplitude $e^-\gamma^* \to e^-\mu^+\mu^-$ for $J_1(e^-_{\lambda_1} \to e^-_{\lambda_3}\mu^+_{\lambda_+}\mu^-_{\lambda_-})$

Now the 4–vector I_μ denotes the current of the $\gamma^* \to \mu^+\mu^-$ transition

$$I_\mu = \bar{u}_-\gamma_\mu v_+ \,. \tag{55}$$

As in Sec. 3.3 it is convenient to replace this current by the 4-vector V_μ without the component along p (compare with Eq. (38))

$$I_\mu \;\to\; V_\mu = I_\mu - \frac{\beta_I}{\beta_l}\, l_\mu = \alpha_V p'_\mu + V_{\perp\mu} \tag{56}$$

because $\beta_V = 2Vp'/s = 0$.

It is easily to see that the vertex factor (54) with its current (55) can be obtained from Eq. (35) and (36) substituting

$$p_+ \to -p_1\,,\;\; p_- \to p_3\,,\;\; k \to -l\,,\;\; M \to m\,,\;\; v_+ \leftrightarrow u_1\,,\;\; \bar{u}_- \leftrightarrow \bar{u}_3\,. \tag{57}$$

This means that the final expression for J_1 can be found from Eq. (47) by the following substitution rules (compare with Eqs. (20)-(21))

$$k^2 \to l^2\,,\;\; M \to m\,,\;\; \mathbf{r}_+ \to \frac{\mathbf{l}_\perp}{x}\;,\;\; \mathbf{r}_- \to \mathbf{q}_\perp - \frac{\mathbf{l}_\perp}{x}\;,$$

$$\beta_+ = x_+ \to -\beta_1 = -1\;,\;\; \beta_- = x_- \to \beta_3 = x_3 \approx 1-x\,,\;\; \beta_k \approx x \to -\beta_l = -x\,, \tag{58}$$

and

$$\lambda \to -\lambda\;,\;\; \lambda_+ \to -\lambda_1\;,\;\; \lambda_- \to \lambda_3\;,\;\; \varphi_{+,-} \to \varphi_{1,3}\;. \tag{59}$$

Using these rules we find (compare with Eq. (47))

$$J_1 = (4\pi\alpha)^{3/2}\,\frac{\sqrt{1-x}}{l^2}\,\mathrm{e}^{i(\lambda_3\varphi_3-\lambda_1\varphi_1)}\times$$

$$\times\left\{\sum_\lambda(\mathbf{V}_\perp\mathbf{e}_\lambda)\left[\left(\frac{2-x}{x}+2\lambda_1\lambda\right)\sqrt{2}\mathbf{Q}\mathbf{e}^*_\lambda\,\delta_{\lambda_1\lambda_3}+2mR\;\delta_{\lambda_1,-\lambda_3}\delta_{\lambda,2\lambda_1}\right]-\right.$$

$$\left.-2\sqrt{2}\,\frac{1-x}{x^3}\,\beta_I R\, l^2\,\delta_{\lambda_1\lambda_3}\right\}\,. \tag{60}$$

where

$$\mathbf{u} = \frac{\mathbf{l}_\perp}{x},\;\mathbf{v} = \mathbf{q}_\perp - \frac{\mathbf{l}_\perp}{x},\;a = m^2+\mathbf{u}^2+\frac{1-x}{x^2}l^2\,,\;b = m^2+\mathbf{v}^2+\frac{1-x}{x^2}l^2 \tag{61}$$

and the quantities $\mathbf{Q}$ and R are given in Eq. (7).

For $l^2 \to 0$ the expression in square brackets in Eq. (60) coincides with the corresponding expression in Eq. (16).

Let us point out that

$$l^2 = (p_+ + p_-)^2 = s(\alpha_+ + \alpha_-)\beta_l - (\mathbf{p}_{+\perp} + \mathbf{p}_{-\perp})^2 = \frac{(x_+\mathbf{p}_{-\perp} - x_-\mathbf{p}_{+\perp})^2 + M^2x^2}{x_+x_-}\,. \quad (62)$$

Note also the useful relation (compare with Eqs. (18) and (45))

$$\mathbf{Q}^2 + \left(m^2 + \frac{1-x}{x^2}\,l^2\right)\,R^2 = \frac{\mathbf{q}_\perp^2}{ab}\,. \quad (63)$$

The result (60) can also be presented with the same accuracy in another form using two-component spinors w_{λ_j} in which we have to set the polar scattering angle θ_3 equal to zero, $\theta_3 = 0$ (compare with Eq. (47))

$$J_1 = \sqrt{2}\,(4\pi\alpha)^{3/2}\frac{\sqrt{1-x}}{l^2}\times$$

$$w^+_{\lambda_3}\left\{\frac{2-x}{x}\,\mathbf{Q}\mathbf{V}_\perp + i\boldsymbol{\sigma}[\mathbf{Q} + mR\,\mathbf{n}_1, \mathbf{V}_\perp] - 2\frac{1-x}{x^3}\,\beta_I\,R\,l^2\right\}\,w_{\lambda_1}\,. \quad (64)$$

The explicitly calculated quantities β_I and $\mathbf{V}_\perp\mathbf{e}_\lambda$ are

$$\beta_I = \frac{2}{s}\,p'_\mu I^\mu = \frac{2}{s}\bar{u}_-\hat{p}'v_+ = 2i\sqrt{x_+x_-}\;\mathrm{e}^{i(\lambda_+\varphi_+ + \lambda_-\varphi_-)}\;\delta_{\lambda_+,-\lambda_-}\,, \quad (65)$$

and

$$\mathbf{V}_\perp\mathbf{e}_\lambda = i\lambda\sqrt{2E_+E_-}\,\mathrm{e}^{i(\lambda_+\varphi_+ + \lambda_-\varphi_-)}\times$$

$$\times\left\{\left[\left(\frac{x_+}{x} - \delta_{\lambda,2\lambda_-}\right)\,\theta_+\mathrm{e}^{i\lambda\varphi_+} + \left(\frac{x_-}{x} - \delta_{\lambda,2\lambda_+}\right)\,\theta_-\mathrm{e}^{i\lambda\varphi_-}\right]\,\delta_{\lambda_+,-\lambda_-} + \right. \quad (66)$$

$$\left.\lambda\left(\frac{M}{E_+} + \frac{M}{E_-}\right)\delta_{\lambda,2\lambda_+}\,\delta_{\lambda_+,\lambda_-}\right\}$$

Eqs. (52)-(53) or (50)-(51) can be obtained from Eqs. (65)-(66) using the rules (58)-(59).

5 Discussion

The main results of our paper are summarised in Eqs. (47) and (60) (combined with (4) and (34)) which give the analytical expressions of all 64 helicity amplitudes for small angle lepton pair production in e^-e^+ or $\mu^-\mu^+$ collisions. Since various distributions of this pair production are well-known (see, for example, reviews [14] and [15]), we briefly discuss only some qualitative features of the obtained results.

1. As for the processes of Figs. 1-4, 7, the obtained formulae are very compact expressions. Additionally, they are convenient for numerical calculations since in their form

large compensating terms are already cancelled. Indeed, the quantities $\mathbf{Q}$ and R, which are defined in Eqs. (7) (with (44) or (61)), and the vertex factors J_1 (47), (60) themselves vanish at small transverse momentum of the t–channel exchange photon $|\mathbf{q}_\perp|$

$$|\mathbf{Q}|,\ R,\ J_1\ \propto |\mathbf{q}_\perp| \ \text{ at } \ |\mathbf{q}_\perp| \to 0\ . \tag{67}$$

Therefore, the amplitude of the process behaves as ((4),(67),(34),(30))

$$M_{fi}\ \propto \frac{|\mathbf{q}_\perp|}{\mathbf{q}_\perp^2 + m^2\alpha_q^2} \ \text{ at } \ |\mathbf{q}_\perp| \to 0\ . \tag{68}$$

Here the mass m denotes that of the colliding lepton.

2. The behaviour of J_1 for two-photon pair production (47) at small $|\mathbf{k}_\perp|$ is mainly determined by the factor $\mathbf{V}_\perp/k^2$. Averaging over the spin states of the initial electron and summing up over the final electron spin we find

$$\frac{1}{2}\sum_{\lambda_1,\lambda_3} V_i V_j^* = \frac{4}{x^2}k_i k_j - k^2\,\delta_{ij};\ \ i,j = x,y \tag{69}$$

from which it follows that

$$|J_1|^2 \propto \frac{(2-2x+x^2)\mathbf{k}_\perp^2 + m^2x^4}{(\mathbf{k}_\perp^2 + m^2x^2)^2} \ \text{ at } \ |\mathbf{k}_\perp| \to 0\ . \tag{70}$$

3. Let us consider the amplitudes for bremsstrahlung pair production which violate electron helicity conservation. They are proportional to (see Eq. (60))

$$m\,R\,\delta_{\lambda_1,-\lambda_3}\,\delta_{\lambda,2\lambda_1}\ . \tag{71}$$

Therefore, in such amplitudes the photon helicity λ is strictly connected with the helicity of the initial electron $\lambda = 2\lambda_1$. The relative magnitude of these amplitudes can be estimated as

$$\frac{|J_1(\lambda_3 = -\lambda_1)|}{|J_1(\lambda_3 = +\lambda_1)|} \sim \frac{xm|R|}{|\mathbf{Q}|}\,. \tag{72}$$

This ratio is small at $m/|\mathbf{p}_{i\perp}|,\ m/|\mathbf{q}_\perp| \ll 1$, i.e. in the region of not very small scattering angles. The same behaviour show the amplitudes which violate muon helicity conservation being proportional to $M\,\delta_{\lambda_+,\lambda_-}\,\delta_{\lambda,2\lambda_+}$.

It is interesting to note that the amplitudes which violate the muon (electron) helicity conservation have a specific dependence on the azimuthal angles. This is true both for the two-photon and bremsstrahlung mechanism: if $\lambda_+ = \lambda_-$ (or $\lambda_1 = -\lambda_3$) then $M_{fi} \sim \exp(i\lambda_+(\varphi_- + \varphi_+))$ (or $\quad M_{fi} \sim \exp(i\lambda_1(\varphi_1 + \varphi_3))$).

4. The two-photon lepton pair production mechanism dominates in the region of soft particle production mentioned in 3.1. The produced leptons have low energies compared with the initial energy E_1, i.e. at $x_\pm \ll 1$. In this region

$$\mathbf{V}_\perp \approx -\frac{\beta_I}{x}\,\mathbf{k}_\perp \tag{73}$$

and the vertex factor J_1 (48) is considerably simplified

$$J_1 = -i\sqrt{2}(4\pi\alpha)^{3/2}\,\frac{\sqrt{x_+x_-}}{x}\,\frac{\beta_I}{k^2}\,w^+_{\lambda_-}\;(A + i\boldsymbol{\sigma}\mathbf{B})\;w_{-\lambda_+}\,,$$

$$A = \frac{x_+ - x_-}{x}\,\mathbf{Q}\mathbf{k}_\perp - 2\,\frac{x_+x_-}{x^2}\,R\,\mathbf{k}^2_\perp\,,\;\; \mathbf{B} = [\mathbf{Q} + MR\,\mathbf{n}_1, \mathbf{k}_\perp]\,. \tag{74}$$

The differential cross section for unpolarised particles is obtained as follows ($i = 1-4, \pm$)

$$d\sigma = \frac{1}{4}\sum_{\lambda_i}\left|\frac{s}{q^2}J_1J_2\right|^2\,\frac{d\Gamma}{2s} = 32\frac{(4\pi\alpha)^4}{(q^2k^2)^2}\frac{x_+x_-}{x^2}\,\left(A^2 + \mathbf{B}^2\right)\,\frac{s}{2}\,d\Gamma\,, \tag{75}$$

where $d\Gamma$ is the phase space of the final particles. Using the relation (45), the expression $A^2 + \mathbf{B}^2$ can be transformed to the symmetric form

$$A^2 + \mathbf{B}^2 = \frac{\mathbf{k}^2_\perp\mathbf{q}^2_\perp}{ab} - \frac{x_+x_-}{x^2a^2b^2}\left\{(\mathbf{k}_\perp\mathbf{q}_\perp)(\mathbf{k}_\perp\mathbf{q}_\perp - \mathbf{p}^2_{+\perp} - \mathbf{p}^2_{-\perp} - 2M^2) + (\mathbf{k}_\perp\boldsymbol{\Delta})(\mathbf{q}_\perp\boldsymbol{\Delta})\right\}^2\,,$$

$$\boldsymbol{\Delta} = \mathbf{p}_{+\perp} - \mathbf{p}_{-\perp} \tag{76}$$

which coincides with Eq. (4.21) in Ref. [15].

Acknowledgements. We are grateful to E. Boos, G. Kotkin and Y. Kurihara for useful discussions. This work is supported in part by Volkswagen Stiftung (Az. No. I/72 302) and by Russian Foundation for Basic Research (code 96-02-19114).

A Definitions of polarised leptonic spinors

A polarisation state of an electron with momentum $\mathbf{p}$, energy $E = \sqrt{\mathbf{p}^2 + m^2}$ and helicity $\lambda = \pm 1/2$ is described by the bispinor

$$u^{(\lambda)}_{\mathbf{p}} = \begin{pmatrix} \sqrt{E+m}\,w^{(\lambda)}_{\mathbf{n}} \\ \sqrt{E-m}\,(\boldsymbol{\sigma}\mathbf{n})\,w^{(\lambda)}_{\mathbf{n}} \end{pmatrix}\,, \qquad \mathbf{n} = \frac{\mathbf{p}}{|\,\mathbf{p}\,|} = (\sin\theta\cos\varphi, \sin\theta\sin\varphi, \cos\theta),$$

where σ are the Pauli matrices and the two-component spinors $w^{(\lambda)}_{\mathbf{n}}$ obey the equations

$$(\boldsymbol{\sigma}\mathbf{n})\,w^{(\lambda)}_{\mathbf{n}} = 2\lambda\,w^{(\lambda)}_{\mathbf{n}}\,,\;\; w^{(\lambda)+}_{\mathbf{n}}w^{(\lambda')}_{\mathbf{n}} = \delta_{\lambda\lambda'}\,,$$

$$w^{(1/2)}_{\mathbf{n}} = \begin{pmatrix} \mathrm{e}^{-i\varphi/2}\cos\frac{\theta}{2} \\ \mathrm{e}^{i\varphi/2}\sin\frac{\theta}{2} \end{pmatrix}\,, \quad w^{(-1/2)}_{\mathbf{n}} = \begin{pmatrix} -\mathrm{e}^{-i\varphi/2}\sin\frac{\theta}{2} \\ \mathrm{e}^{i\varphi/2}\cos\frac{\theta}{2} \end{pmatrix}\,.$$

The normalisation conditions are

$$\bar{u}^{(\lambda)}_{\mathbf{p}}u^{(\lambda')}_{\mathbf{p}} = 2m\,\delta_{\lambda\lambda'}\,, \qquad \sum_\lambda u^{(\lambda)}_{\mathbf{p}}\bar{u}^{(\lambda)}_{\mathbf{p}} = \hat{p} + m\,.$$

For positrons the corresponding formulae read

$$v^{(\lambda)}_{\mathbf{p}} = -2\lambda i\begin{pmatrix} \sqrt{E-m}\,(\boldsymbol{\sigma}\mathbf{n})\,w^{(-\lambda)}_{\mathbf{n}} \\ \sqrt{E+m}\,w^{(-\lambda)}_{\mathbf{n}} \end{pmatrix},$$

$$\bar{v}^{(\lambda)}_{\mathbf{p}} v^{(\lambda')}_{\mathbf{p}} = -2m\,\delta_{\lambda\lambda'}\,, \quad \sum_{\lambda} v^{(\lambda)}_{\mathbf{p}} \bar{v}^{(\lambda)}_{\mathbf{p}} = \hat{p} - m\,.$$

In the paper we also use the short notations $u_j = u^{(\lambda_j)}_{\mathbf{p}_j}$, $v_j = v^{(\lambda_j)}_{\mathbf{p}_j}$ and $w_{\lambda_j} = w^{(\lambda_j)}_{\mathbf{n}_j}$. For the initial electron with momentum $\mathbf{p}_1$ along the z-axis we put $\theta = \varphi = 0$, for the initial positron with $\mathbf{p}_2$ opposite to the z-axis $\theta = \pi\,,\ \varphi = 0$. For the final positron with momentum $\mathbf{p}_4$ $\theta = \pi - \theta_4$ and $\varphi = \varphi_4$ are used.

References

[1] V.N. Baier, V.M. Galitsky: Phys. Lett. **13**, 355 (1964); Zh. Exp. Teor. Fiz. **49**, 661 (1964)

[2] P.I. Golubnichy et al.: Atomnaya Energ. **22**, 168 (1966)

[3] I. Augustin et al.: Preprint LAL-1249 (1971)

[4] G. De Zorzi et al.: Polarization at LEP, Preprint CERN 88-06, v. 2, p. 64 (1988)

[5] G.L. Kotkin, S.I. Polityko, A. Schiller, V.G. Serbo: Phys. Lett. **B221**, 96 (1989)

[6] C. Bini et al.: Nucl. Instr. Methods **A 349**, 27 (1994)

[7] A. Courau, G. Pancheri: Phys. Lett. **B 396**, 287 (1997)

[8] I.F. Ginzburg, G.L. Kotkin, V.G. Serbo, V.I. Telnov: Pisma ZhETF **34**, 514 (1981); Nucl. Instr. Methods **205**, 47 (1983)

[9] E.A. Kuraev, A. Schiller, V.G. Serbo: Phys. Lett. **B134**, 455 (1984)

[10] E.A. Kuraev, A. Schiller, V.G. Serbo: Nucl. Phys. **B 256**, 189 (1985)

[11] $\mu^+\mu^-$ Collider: A Feasibility Study: Preprint BNL-52503 (1996)

[12] I.F. Ginzburg: Nucl. Phys. B (Proc. Suppl.) **51A**, 196 (1996)

[13] I.F. Ginzburg, S.L. Panfil and V.G. Serbo: Nucl. Phys. **B 284**, 685 (1987) and **B 296**, 581 (1988); I.F. Ginzburg and D.Yu. Ivanov: Nucl. Phys. **B 388**, 376 (1992)

[14] V.M. Budnev, I.F. Ginzburg, G.V. Meledin and V.G. Serbo: Phys. Rep. **15C**, 181 (1975)

[15] V.N. Baier, B.S. Fadin, V.A. Khoze and E.A. Kuraev: Phys. Rep. **78**, 293 (1981)

[16] A.B. Arbuzov et al.: Phys. Lett. **B 394**, 218 (1997)

[17] R. Kleiss: Nucl. Phys. **B 241**, 61 (1984); F.A. Berends et al.: Nucl. Phys. **B 264**, 243 (1986)

[18] V.S. Fadin, E.A. Kuraev, A.N. Peryshkin: Preprint INP 86-91 (Novosibirsk, 1986); E.A. Kuraev, A.N. Peryshkin: Yadernaya Fizika **42**, 1195 (1986)

[19] E.A. Kuraev, A. Schiller, V.G. Serbo: Z. Phys. **C 30**, 237 (1986)

[20] A.I. Akhiezer, V.B. Berestetskii: Quantum electrodynamics (Moscow: Nauka, 1981)

[21] E.A. Kuraev, L.N. Lipatov and M.I. Strikman: Zh. Eksp. Teor. Fiz. **66**, 838 (1974)